Proceedings of the Design Society, Volume 5: ICED25
https://doi.org/10.1017/pds.2025.10262

Modeling Stochastic Yield Rates in Disassembly Processes for Green Profit Maximization

Yilan Jiang and Harrison Kim,✉

Department of Industrial and Enterprise Systems Engineering, University of Illinois Urbana-Champaign, Illinois, USA

✉ hmkim@illinois.edu

ABSTRACT: Many optimization models have been proposed to assist original equipment manufacturers (OEMs) in pricing and production planning for remanufactured product; however, most assume deterministic yield rates for takeback products during disassembly. In practice, yield rates are influenced by interdependencies among subparts and disassembly operations. To address this limitation, this study enhances a previously established optimization approach by incorporating yield uncertainty into the disassembly process using a diffusion process framework. The effectiveness of this approach is validated through case studies on two distinct products: a smartphone and a recreational boat engine. The results demonstrate that integrating stochastic yield modeling allows stakeholders to make more informed decisions, ultimately improving both economic performance and environmental sustainability.

KEYWORDS: stochastic optimization, quality uncertainty, sustainable design

1. Introduction

In 2021, the manufacturing sector contributed 72% of U.S. industrial carbon emissions, the highest among all industrial components (CBO, 2023). In light of global carbon neutrality goals (European Parliament, 2019), it is crucial for original equipment manufacturers (OEMs)—key players in the manufacturing sector—to actively reduce their carbon footprint. Remanufacturing, which restores end-of-life (EoL) products using reused, repaired, and new parts, is a key sustainable design strategy that reduces carbon emissions and increases revenue (Kwak, 2012; Johnson and McCarthy, 2014).

To successfully integrate remanufactured products into OEMs' production lines, various decisionmaking tools have been proposed to optimize production and marketing strategies, maximizing revenue while minimizing environmental impact (Kwak and Kim, 2017, Kwak, 2018). While optimization models improve remanufacturing decisions, complementary strategies also play a vital role. Modular design (Fadeyi and Monplaisir, 2022) enhances disassembly, predictive maintenance (Zhang et al., 2022) extends product lifespan, and AI-driven quality assessment (Schlüter et al., 2021) improves sorting and processing efficiency. Together, these strategies strengthen the economic and environmental benefits of remanufacturing.

Accurately modeling end-of-life (EoL) product quality is key to maximizing material recovery and minimizing costs (Stamer and Sauer, 2024). For instance, diesel engine remanufacturing cuts CO_2 emissions by 74% compared to new manufacturing (Dias et al., 2013), and marine sector remanufacturing can save up to 40,000 tons of CO_2 annually in the EU (Wahab et al., 2018). The modeling of EoL product quality has been extensively explored in remanufacturing research, with Panagiotidou et al. (2013) identifying two widely used indicators for assessing take-back core quality: proportional yield (fraction of remanufacturable components) and continuous yield rate (reusability of individual cores) (Zikopoulos and Tagaras, 2007; Galbreth and Blackburn, 2010). While the latter is more precise, data collection is challenging without disassembly (Yang et al., 2015).

This study models EoL quality through yield rates at each disassembly operation, refining previous approaches (Kwak and Kim, 2017). Rather than assessing an entire core, it examines disassembly-level yield rates for a more granular representation. Furthermore, to account for variability and uncertainty, this study incorporates yield uncertainty into the disassembly process using a diffusion process approach (Sohl-Dickstein et al., 2015). This stochastic framework captures variability across disassembly levels, improving OEM decision-making and enhancing both economic and environmental outcomes. The key contributions of this paper can be summarized as follows:

- This research introduces a diffusion-based framework for modeling yield uncertainty in disassembly processes. It captures stochastic yield rates across multiple disassembly levels and integrates seamlessly into optimization models. This flexible, generalizable approach addresses yield variability, a critical yet often overlooked aspect of disassembly optimization.
- The framework extends the green profit maximization model of Kwak and Kim (2017) by incorporating stochastic yield rates for greater realism. While this study applies the framework specifically to extend Kwak and Kim (2017), the yield uncertainty modeling is designed to be flexible and broadly applicable to various EoL optimization problems. Its effectiveness is validated through two case studies: (i) smartphone disassembly, tested in the original deterministic model, and (ii) Brunswick boat engine disassembly. Results show that modeling yield uncertainty improves decision-making, enhancing both economic outcomes and environmental sustainability.

2. Literature Review

This section reviews key studies relevant to the proposed framework. Section 2.1 examines yield rate modeling in disassembly, highlighting both deterministic and stochastic approaches. Section 2.2 discusses diffusion processes, which inspire the stochastic modeling framework used in this study. Section 2.3 explores sustainable design strategies, including optimization-based decision tools and broader approaches that enhance remanufacturing efficiency and disassemblability.

2.1. Yield Rate Modeling in Disassembly

Existing research on yield rate modeling in disassembly processes can be broadly classified into two approaches: deterministic and stochastic modeling. Deterministic yield models assume fixed yield rates for all take-back products. For instance, Kwak and Kim (2017) used a transition matrix with predefined, constant yield rates for production planning. While simplifying modeling, this approach demands simultaneous yield rate inputs, making it time-consuming and often unrealistic. Similarly, Huang et al. (2018) classified used products into three quality grades—high, medium, and low—using modal intervals. While this method introduces quality uncertainty, yield rates within each grade remain deterministic, failing to capture real-world variability.

Disassembly involves multiple stakeholders—OEMs, third-party remanufacturers, and logistics providers—who influence core recovery. Priyono et al. (2016) outlined key disassembly stages: inspection, sorting, selective disassembly, and cleaning, all of which impact yield variability. Effective stakeholder coordination enhances disassembly efficiency, improving material recovery while reducing economic and environmental costs.

Stochastic models address disassembly uncertainty by representing take-back core quality probabilistically. Yang et al. (2015) modeled core quality distributions, considering remanufacturing time. Other studies explored exponential and Weibull distributions (Kumar, 2014; Ke et al., 2009). Despite capturing yield uncertainty, these methods overlook interdependencies across disassembly levels. Further exploration of uncertainty propagation could provide a more realistic representation.

2.2. Diffusion Process

Diffusion models, first introduced by Sohl-Dickstein et al. (2015), are deep generative frameworks originally designed for image generation but now widely used in constrained optimization (Ho et al., 2020, Mazé and Ahmed, 2022). The diffusion process, denoted as q, represents the forward step, where noise is added iteratively via a Markov chain to transform data into a noise-like distribution. A variance schedule β_t controls the noise at each time step t, as formulated in Equation 1:

$$q(x_t|x_{t-1} = \mathcal{N}(x_t; \sqrt{\beta_t}x_{t-1}, (1 - \beta_t\mathbb{I})) \tag{1}$$

where $\mathcal{N}$ is a Gaussian distribution, x_t is the data state at time t, and $\mathbb{I}$ is the identity matrix. This process gradually deconstructs the data structure into pure noise.

The diffusion process effectively models yield rate variability and sequential dependencies in disassembly. Yield rates are stochastic, influenced by take-back quality, efficiency, and subpart conditions. By introducing controlled noise at each step, this Markov chain-based approach aligns with the hierarchical nature of disassembly, where each level's yield rate depends on the previous one. The variance schedule further allows stakeholders to adjust variability for specific products, making diffusion modeling a flexible tool for remanufacturing.

2.3. Sustainable Design

Sustainable design balances economic, environmental, and social factors by integrating resourceefficient practices into production. In remanufacturing, studies have optimized demand, supply, core acquisition, and production to support OEMs, retailers, and policymakers (Kwak and Kim, 2017, Kwak, 2018, Sun and Li, 2023). Beyond economic and operational optimization, sustainable design enhances disassemblability and remanufacturing efficiency. Ijomah et al. (2007) proposed design-for-remanufacturing (DfR) guidelines to improve component recovery and reduce costs. Ijomah (2009) addressed decision-making challenges in remanufacturing, advocating structured design approaches to enhance take-back core quality. Dong et al. (2006) introduced a hierarchical disassembly planning approach using a hierarchical attributed liaison graph (HALG) to improve remanufacturing efficiency while reducing computational complexity. These studies highlight sustainable design's role in shaping remanufacturing strategies and take-back core quality. Additionally, Life Cycle Assessment (LCA) is widely used to assess remanufacturing's sustainability benefits (Zheng et al., 2019, Zhang et al., 2020), and this study derives its environmental impact parameters from LCA calculations.

These studies underscore sustainable design's impact on remanufacturing and take-back core quality. Among them, Kwak and Kim (2017) developed a mixed-integer nonlinear programming (MINLP) model integrating pricing, production, and environmental considerations for new and remanufactured products. The study assumes deterministic yield rates for the disassembly process, represented in the form of a transition matrix, as illustrated in Figure 1.

In Figure 1, the letters in parentheses represent the component condition: '(R)' denotes 'remanufactured', 'W' denotes 'working' and 'N' denotes 'not-working'. Operations 1 to 4 represent disassembly operations. For example, in operation 1, an EoL product ABC is taken as input, producing 70% working AB, 30% not-working AB, 90% working component C and 10% not-working component C. These proportion of reusable parts (i.e. 0.7 and 0.9) are referred to as yield rates.

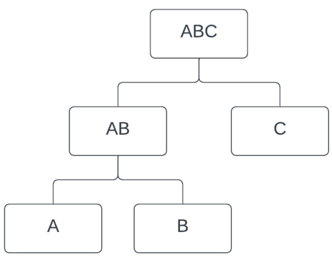

		Operation j						
		1	2	3	4	5	6	7
1	Product ABC (R)							1
2	Product ABC (EOL 1)	-1						
3	Subassembly AB (R)							-1
4	Subassembly AB (W)	0.7	-1				1	
5	Subassembly AB (N)	0.3						
6	Component A (R)			1			-1	
7	Component B (R)				1		-1	
8	Component C (R)					1		-1
9	Component A (W)		0.2	-1				
10	Component B (W)		0.6		-1			
11	Component C (W)	0.9				-1		
12	Component A (N)		0.8					
13	Component B (N)		0.4					
13	Component C (N)	0.1						

Figure 1. Disassembly structure of example product ABC and its corresponding transition matrix (Kwak and Kim, 2017)

3. Methodology

The proposed methodology integrates yield uncertainty modeling into an optimization framework to enhance sustainable product design and remanufacturing. Disassembly, a key process in end-of-life (EoL) product management, maximizes material recovery and minimizes environmental impact. Section 3.1 introduces the yield uncertainty modeling approach, Section 3.2 presents the stochastic model extending Kwak and Kim (2017), and Section 3.3 outlines the numerical algorithm for scenario generation and reduction.

3.1. Yield Dependency Modeling in Disassembly

Previous studies (Lambert, 2002; Kwak et al., 2009; Kang et al., 2010; Kwak and Kim, 2017) have commonly used transition matrices (Figure 1) to represent the relationship between product design and remanufacturing operations. Remanufacturing typically involves three stages: disassembly, reconditioning, and reassembly. This study focuses on the disassembly stage, as the quality of EoL products is inherently uncertain when collected by third-party takeback companies. It is assumed that a third-party company gathers used products from customers, and the OEM repurchases these products from the third party, with the buyback price determined in this study.

Given an EOL product, let $t = \{0,1,2, ..., T\}$ represent the disassembly levels, and let $\{y_t\}_{t=0}^{T}$ denote the sequence of random variable corresponding to the yield rates at each disassembly level. For simplicity, it is assumed that all parts within a given disassembly level share the same yield rate. while this assumption can be relaxed to follow distinct yield rates for each part, it is adopted in this study for demonstration purposes.

At $t = 0$, y_0 represents the yield rate of the initial disassembly level and is modeled as a truncated normal distribution, $y_0 \sim \mathcal{N}(\mu_0, \sigma_0^2)$, truncated to the interval [0,1]. A third-party takeback company assesses the EOL product and provides the OME with a rough quality score ranging from 0 to 1, which serves as μ_0. The variance σ_0^2 is determined by the OEM's production planning experts based on domain knowledge and historical data.

For subsequent disasembly levels ($t \geq 0$), the OEM defines a sequence of variance schedule, $\{\beta_t\}_{t=1}^{T}$, to control the variabilioty of yield rates at each level. At disassembly level t, the yield rate y_t is modeled as a conditional truncated normal distribution, dependent on the previous yield rate y_{t-1}, as expressed in Equation 2.

$$q(y_t|y_{t-1}) = \mathcal{N}(y_t; \sqrt{\beta_t} x_{t-1}, (1 - \beta_t)) \tag{2}$$

The use of the variance schedule $\{\beta_t\}_{t=1}^{T}$ provides OEM experts with the flexibility to adapt the model to specific disassembly cases. This formulation, inspired by diffusion processes, assumes that the yield rate at each level depends only on the yield rate at the preceding level, consistent with the properties of a Markov process. This assumption is reasonable, as the yield rate of a subassembly or part naturally depends on the quality observed at the upper disassembly level (Darghouth and Abdel-Aal, 2021).

3.2. Model Formulation

Since yield rates at each disassembly level are stochastic, the mixed-integer programming model from Kwak and Kim (2017) is revised to maximize expected profit:

$$\max \mathbb{E}_Y[\text{Profit}(P_n, Z_n, P_r, Z_r, M_i, N_i, P_k, X_k, O_j)], \tag{3}$$

where $\mathbb{E}_Y$ represents the expectation over stochastic yield rates $\{y_t\}_{t=0}^{T}$, and Profit$(\cdot)$ follows Equation 4 from Kwak and Kim (2017). The decision variables are:

- P_n, Z_n: Selling price and production volume of new products.
- P_r, Z_r: Selling price and production volume of remanufactured products.
- P_k, X_k: Buyback price and return volume of end-of-life product k ($\forall k \in K$).
- M_i, N_i, O_i: Recycling volume, new part production ($\forall i \in I$), and operation frequency ($\forall j \in J$).

The profit function for a single-period production horizon is:

$$\begin{aligned}\text{Profit}(P_n, Z_n, P_r, Z_r, M_i, N_i, P_k, X_k, O_j) = (P_n - C_n)Z_n + P_r Z_r \\ -(\sum_{i\in I} c_i^M M_i + \sum_{k\in K} P_k X_k + \sum_{j\in J} c_j O_j + \sum_{i\in I} c_i^N N_i + c_d Z_r)\end{aligned} \tag{4}$$

The model maintains constraints on production capacities, disassembly flow balances, and green profit thresholds, consistent with Kwak and Kim (2017). For full constraint details, refer to their work. The numerical solution method is described in Section 3.3.

Environmental impact is assessed through carbon savings, measured as the reduction in CO_2 emissions from remanufacturing versus new production. This metric, widely used in sustainability assessments and regulations, was chosen for its standardization. Other factors (e.g., resource depletion, water usage, material recovery) are important but beyond this study's scope (Zhang et al., 2020).

3.3. Numerical Method

The model formulation described in Section 3.2 introduces significant complexity in solving the problem. Even the deterministic version is a nonlinear mixed-integer optimization problem, which requires considerably more computational resources compared to linear programming. Incorporating yield dependency modeling in the disassembly step further complicates the problem, as all decision variables depend on random variables, and the interdependencies among these variables make the problem even less tractable. To address this challenge, this study employs a numerical approach called Scenario Generation, as outlined in Algorithm 3.3.

In Algorithm 3.3, Monte Carlo simulation is employed to generate an initial set of N scenarios (Mooney, 1997), with N set to 100,000 to comprehensively capture yield rate variability. For each scenario, yield rates $\{y_t\}_{t=0}^{T}$ are sampled based on predefined parameters: the initial yield mean (μ_0), initial standard deviation (σ_0), and variance schedule ($\{\beta_t\}_{t=1}^{T}$). To balance computational efficiency and accuracy, k-means clustering (Sinaga and Yang, 2020) is subsequently applied to select K representative scenarios, from which the empirical expected profit is calculated.

Scenario Generation Algorithm [1] Initial yield mean μ_0, initial yield standard deviation σ_0, variance schedule ($\{\beta_t\}_{t=1}^{T}$), truncation bounds [0,1], number of initial scenarios N, number of reduced scenarios K Reduced set of scenarios $\{\mathbf{Y}^{(1)}, \mathbf{Y}^{(2)}, \ldots, \mathbf{Y}^{(K)}\}$ with estimated joint probabilities $\{P^{(1)}, P^{(2)}, \ldots, P^{(K)}\}$ Initialize an empty list of scenarios $n = 1$ to N Generate N initial scenarios Sample initial yield $Y_0 \sim$ TruncatedNormal(μ_0, σ_0, [0,1]) $t = 1$ to T Generate yields for each level Set standard deviation $\sigma_t = 1 - \beta_t$ Sample $Y_t \sim$ TruncatedNormal ($\sqrt{\beta_t} Y_{t-1}, \sigma_t$, [0.1]) based on previous yield Y_{t-1} Store yield sequence as a scenario

Use k-means clustering to reduce scenarios to K representative scenarios Calculate joint probabilities for each reduced scenario

Reduced scenarios with joint probabilities

To compute the empirical expected profit using the K representative scenarios, the joint probability distribution for each scenario k K is required. Given the Markov property in the diffusion process, the joint distribution for a scenario k can be expressed as:

$$P^{(k)} = q^k(y_0, y_1 \ldots, y_T) = q(y_0) \prod_{t=1}^{T} q(y_t | y_{t-1}), \tag{5}$$

where $q(y_0)$ is defined as the truncated normal distribution: $q(y_0)$ = TruncatedNormal(μ_0, σ_0, [0,1]). Algorithm 3.3 outputs a set of K representative scenarios along with their corresponding joint probabilities. These scenarios serve as realized data points to be input into the MINLP problem, transforming it into a deterministic version for each scenario k. The empirical expected profit is then computed using Equation 6:

$$\mathbb{E}_Y[\text{Profit}(\cdot)] = \sum_{k \in K} P^{(k)} \text{Profit}^{(k)}(\cdot), \tag{6}$$

where $P^{(k)}$ is the joint probability of scenario k, and Profit$^{(k)}(\cdot)$ represents the profit evaluated for scenario k. This numerical approach balances computational efficiency with the need to account for stochastic yield rates in the optimization process.

4. Case Illustrations

In this section, two case studies—a smartphone and a recreational boat engine—are presented to evaluate the effectiveness of the proposed stochastic methodology. Section 4.1 outlines the model assumptions, parameters, and scenarios. Section 4.2 presents the optimization results for each scenario. Finally, Section 4.3 provides a detailed discussion of the optimization results.

4.1. Model Setup

This study evaluates two distinct product types—smartphones and recreational boat engines—to demonstrate the proposed stochastic methodology's effectiveness in OEM decision-making. These products differ in production scale, market size, EoL availability, and remanufacturing processes, providing a comprehensive comparison.

Smartphones are mass-produced with high EoL availability and mature takeback systems. Their disassembly process is relatively simple, involving three levels and 23 operations. In contrast, recreational boat engines serve a niche market with fewer EoL products and a less developed remanufacturing business. Their disassembly process is more complex, assuming five levels and 122 operations (details withheld for confidentiality).

These contrasting characteristics make smartphones and boat engines ideal case studies for evaluating the methodology's robustness across different remanufacturing environments. Table 1 summarizes model assumptions, with smartphone data from Kwak and Kim (2017) and boat engine data based on Brunswick Corporation. Due to confidentiality, boat engine parameters are withheld, and results are normalized.

Table 1. Model Assumptions for Smartphone and Boat Engine

	Smartphone	Boat Engine
Data Sources	Derived from Kwak and Kim (2017)	Brunswick Corporate (normalized for confidentiality)
EoL Product Supply	Two types of EoL products: good and poor	One type of EoL product: relatively good
Demand Assumptions	3 competitors, 3 customer segments	3 competitors, 2 customer segments
Product Design and Operations	3 disassembly levels, 23 remanufacuring operations	5 disassembly levels, 122 remanufacutring operations

Given the two product types and their model assumptions, two scenarios are analyzed:

- Baseline Case: Yield rates are uniform across disassembly levels. For smartphones, EoL product type 1 has a deterministic yield of 1.0, while type 2 is 0.5. For boat engines, the yield for EoL product type 1 is 0.8.
- Stochastic Case: Yield rates vary across disassembly levels. Table 2 summarizes the yield dependency modeling parameters. For smartphones, only the yield rate of the *poor* EoL product type is stochastic, while the *good* type remains deterministic. Three sub-cases assess the methodology's accuracy with 10, 100, and 1000 generated scenarios.

Table 2. Model Parameters for Smartphone and Boat Engine

Parameter	Symbol	Smartphone	Boat Engine
Initial Yield Mean	μ_0	0.5 (Poor EoL)	0.8
Initial Yield Standard Deviation	σ_0	0.1	0.05
Number of Initial Scenarios	N	100,000	100,000
Number of Disassembly Levels	$T+1$	3	5
Variance Schedule	$\{\beta_t\}_{t=1}^{T}$	{0.97,0.98}	{0.92,0.95,0.97,0.98}
Number of Reduced Scenarios	K	{10,100,1000}	{10,100,1000}

4.2. Optimization results

This section presents optimization results for both cases. All problems were solved using the Gurobi Python API under an academic license (Gurobi Optimization, LLC, 2024). Table 3 summarizes the baseline case, where yield rates are deterministic and uniform across disassembly operations. For smartphones, the optimal total profit is \$2.16 million, with environmental savings of 73,767 kg CO_2 equivalent. For boat engines, values are normalized (0 to 100), with an optimal total profit of \$69 and environmental savings of 47.07 kg CO_2 equivalent.

Table 3. Optimization results for the baseline case

	Smartphone	Boat Engine (normalized)
Buyback price	\$61 (Good); \$32 (Poor)	\$39
Takeback quantity	1025 units (Good); 1632 units (Bad)	40 units
Selling price	\$675 (new); \$483 (remanufactured)	\$100 (new); \$85 (remanufactured)
Production quantity	3010 units (new); 2249 units (remanufactured)	100 units (new); 9 units (remanufactured)
Total profit	\$2157,736	\$69
Environmental-impact saving	73,767 $kg\ CO_2$ equivalent	47.04 $kg\ CO_2$ equivalent

Figures 2 and 3 illustrate the stochastic results obtained using the proposed methodology for the three sub-cases introduced in Section 4.1. The 'x' symbols represent the baseline values, as shown in Table 3.

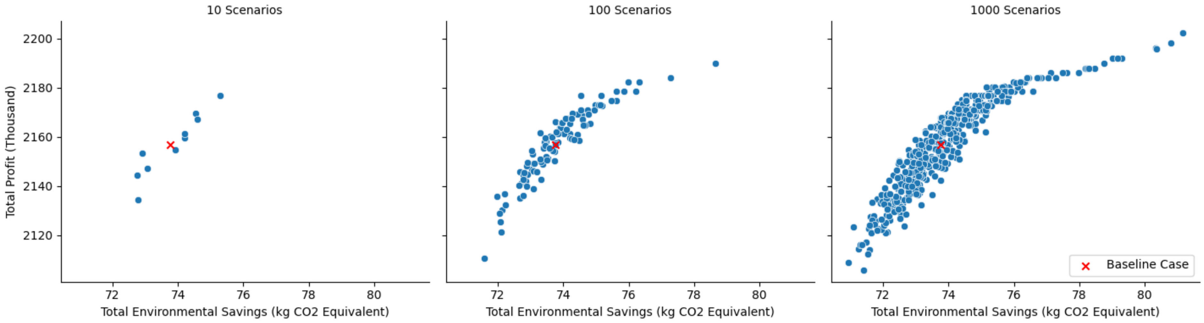

Figure 2. Stochastic Distribution of Total Profit and Environmental Savings Across Different Numbers of Scenarios for Smartphones

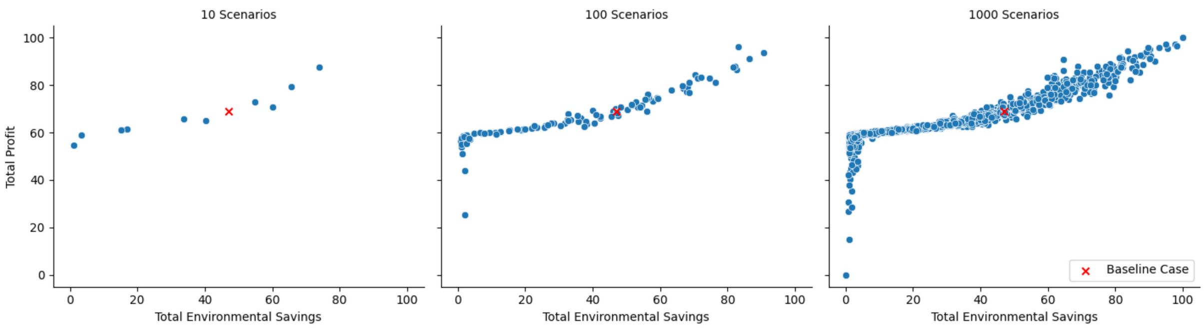

Figure 3. Stochastic Distribution of Total Profit and Environmental Savings Across Different Numbers of Scenarios for Boat Engines

For smartphones, in the 1000-scenario sub-case, 43% of scenarios achieve higher total profit and greater environmental savings than the baseline. Similarly, for boat engines, 33% of scenarios exceed the baseline in both metrics. The total profit distributions under 1000 scenarios follow a normal distribution at a 5% significance level, validated by the Anderson-Darling test.

Moreover, for smartphones, the expected total profit is \$2.157 million (10 scenarios), \$2.159 million (100 scenarios), and \$2.157 million (1000 scenarios). For boat engines, it is \$68.24 (10 scenarios), \$67.88 (100 scenarios), and \$67.86 (1000 scenarios). The consistency across sub-cases highlights the effectiveness of using fewer scenarios with the k-means clustering algorithm, which efficiently captures possible outcomes while maintaining accuracy.

4.3. Discussions

The optimized results in Section 4.2 highlight the benefits of incorporating yield uncertainty into the proposed methodology. While the baseline results provide reasonable estimates of total profit and environmental savings (as 'x' markers are centrally located within the joint distributions), they lack insight into the range of possible operational outcomes. By adopting the stochastic methodology, the model becomes more robust to real-world variations in disassembly, reducing the risk of suboptimal remanufacturing planning.

The stochastic approach gives OEMs critical insights into outcome variability for both new and remanufactured products, which the deterministic baseline does not capture. For smartphones, total profit varies minimally (±2%) due to a stable market and standardized processes, whereas environmental savings fluctuate more significantly (from 10% higher to 3% lower than baseline). These results suggest that OEMs could leverage stable profits and environmental benefits to integrate carbon-saving metrics into long-term planning, such as regulatory compliance, eco-conscious marketing, or carbon credit strategies (Wang et al., 2024).

In contrast, boat engines exhibit greater variability, with total profit ranging from +10% to -22% and environmental savings from +85% to -75% relative to baseline. This results from higher disassembly complexity, greater remanufacturing costs, and sensitivity to initial yield rates. When a take-back engine's overall yield rate falls below 0.5, the model may opt against remanufacturing, amplifying environmental savings variability. These findings emphasize the need for high-quality take-back cores, reinforcing the roles of DfRem and AI-driven condition assessment in reducing variability and enhancing remanufacturing viability (Ijomah et al., 2007). For high-value goods like boat engines, adaptive disassembly strategies that account for yield uncertainty can help OEMs optimize cost-benefit trade-offs in remanufacturing (Priyono et al., 2016).

These insights align with the products' intrinsic differences. Smartphone remanufacturing ensures stable profitability with moderate carbon savings, making it suitable for sustainability-driven policies. Conversely, boat engine remanufacturing has a higher environmental impact but requires an adaptive approach due to yield uncertainty. As carbon savings become increasingly monetized, accounting for variability in disassembly outcomes is essential when formulating remanufacturing strategies.

5. Conclusion

This study introduced yield dependency modeling in disassembly using a diffusion process, integrating it into the framework of Kwak and Kim (2017). Two case studies—a smartphone and a boat engine—demonstrated its adaptability and ability to capture yield variability across disassembly levels, providing decision-makers with more informed outcomes.

Despite its advantages, the framework has limitations. Introducing stochastic elements increases computational complexity, requiring a balance between accuracy and efficiency. Additionally, this study assumes uniform yield rates at each disassembly level, whereas real-world variations exist. Future work could refine part-specific yield modeling for greater accuracy. Additional research could explore alternative optimization approaches, such as hybrid AI-heuristic methods for complexity reduction and contextual optimization based on decision-maker preferences (Sadana et al., 2024). Additionally, integrating ecosystem modeling may enhance coordination among remanufacturing stakeholders (Geary et al., 2020).

While the Markov assumption ensures tractability, real-world disassembly may involve batch-level variations and external disruptions. Future research could investigate non-Markovian approaches, such as reinforcement learning (Sutton et al., 1999), to better model these complexities. Additionally, degradation factors like material fatigue, handling damage, and supplier quality variability could be incorporated using degradation models or machine-learning-based quality predictions. Empirical comparisons between stochastic and deterministic approaches would further validate the model's effectiveness.

While carbon savings provide a widely used sustainability metric, future research could incorporate broader environmental indicators, such as material circularity (MacArthur et al., 2019) and energy efficiency (Finkbeiner et al., 2006), for a more comprehensive evaluation.

Acknowledgments

We would like to express our sincere thanks to Brunswick Corporate (BC) for supporting our work.

References

Congressional Budget Office (CBO) (2023). The long-term budget outlook. *Congressional Budget Office*, Retrieved from https://www.cbo.gov/publication/60030#_idTextAnchor072.

Darghouth, M. N. and Abdel-Aal, M. (2021). A capacitated disassembly scheduling problem considering processing technology selection and parts commonality. *Journal of Remanufacturing*, 11(3), 243–261. Springer.

Dong, T., Zhang, L., Tong, R., and Dong, J. (2006). A hierarchical approach to disassembly sequence planning for mechanical product. *The International Journal of Advanced Manufacturing Technology*, 30, 507–520. Springer.

Dias, A. S., Kim, H., Sivakumar, P. K., Liu, Z.-C., and Zhang, H.-C. (2013). Life cycle assessment: A comparison of manufacturing and remanufacturing processes of a diesel engine. *In Re-engineering Manufacturing for Sustainability: Proceedings of the 20th CIRP International Conference on Life Cycle Engineering, Singapore, 17-19 April, 2013* (pp. 675–678). Springer.

European Parliament (2019). What is carbon neutrality, and how can it be achieved by 2050. *European Parliament*, Retrieved from https://www.europarl.europa.eu/topics/en/article/20190926STO62270/what-is-carbon-neutrality-and-how-can-it-be-achieved-by-2050.

MacArthur, E., Heading, H., *et al.* (2019). How the circular economy tackles climate change. *Ellen MacArthur Foundation*, 1, 1–71.

Finkbeiner, M., Inaba, A., Tan, R., Christiansen, K., and Klüppel, H.-J. (2006). The new international standards for life cycle assessment: ISO 14040 and ISO 14044. *The International Journal of Life Cycle Assessment*, 11, 80–85. Springer.

Fadeyi, J. A. and Monplaisir, L. (2022). Instilling lifecycle costs into modular product development for improved remanufacturing-product service system enterprise. *International Journal of Production Economics*, 246, 108404. Elsevier.

Galbreth, M. R. and Blackburn, J. D. (2010). Offshore remanufacturing with variable used product condition. *Decision Sciences*, 41(1), 5–20. Wiley Online Library.

Galbreth, M. R. and Blackburn, J. D. (2010). Optimal acquisition quantities in remanufacturing with condition uncertainty. *Production and Operations Management*, 19(1), 61–69. SAGE Publications Sage CA: Los Angeles, CA.

Geary, W. L., Bode, M., Doherty, T. S., Fulton, E. A., Nimmo, D. G., Tulloch, A. I. T., Tulloch, V. J. D., and Ritchie, E. G. (2020). A guide to ecosystem models and their environmental applications. *Nature Ecology & Evolution*, 4(11), 1459–1471. Nature Publishing Group UK London.

Gurobi Optimization, LLC (2024). *Gurobi Optimizer Reference Manual*. Available at: https://www.gurobi.com.

Ho, J., Jain, A., and Abbeel, P. (2020). Denoising diffusion probabilistic models. *Advances in Neural Information Processing Systems*, 33, 6840–6851.

Huang, M., Yi, P., Shi, T., and Guo, L. (2018). A modal interval based method for dynamic decision model considering uncertain quality of used products in remanufacturing. *Journal of Intelligent Manufacturing*, 29, 925–935. Springer.

Ijomah, W. L. (2009). Addressing decision making for remanufacturing operations and design-for-remanufacture. *International Journal of Sustainable Engineering*, 2(2), 91–102. Taylor & Francis.

Ijomah, W. L., McMahon, C. A., Hammond, G. P., and Newman, S. T. (2007). Development of design for remanufacturing guidelines to support sustainable manufacturing. *Robotics and Computer-Integrated Manufacturing*, 23(6), 712–719. Elsevier.

Johnson, M. R. and McCarthy, I. P. (2014). Product recovery decisions within the context of extended producer responsibility. *Journal of Engineering and Technology Management*, 34, 9–28. Elsevier.

Kang, C. M., Kwak, M. J., Cho, N. W., and Hong, Y. S. (2010). Automatic derivation of transition matrix for end-of-life decision making. *International Journal of Production Research*, 48(11), 3269–3298. Taylor & Francis.

Ke, J.-C., Su, Z.-L., and Wang, K.-H. (2009). An availability system with general repair distribution: statistical inference. *Communications in Statistics-Theory and Methods*, 38(9), 1508–1525. Taylor & Francis.

Kumar, D. (2014). Quotient moments of the Erlang-Truncated Exponential distribution based on record values and a Characterization. *Journal of Applied Mathematics & Informatics*, 32(1_2), 7–16. The Korean Society for Computational and Applied Mathematics.

Kwak, M. (2012). *Green Profit Design for Lifecycle*. University of Illinois at Urbana-Champaign.

Kwak, M. and Kim, H. (2017). Green profit maximization through integrated pricing and production planning for a line of new and remanufactured products. *Journal of Cleaner Production*, 142, 3454–3470. Elsevier.

Kwak, M. J., Hong, Y. S., and Cho, N. W. (2009). Eco-architecture analysis for end-of-life decision making. *International Journal of Production Research*, 47(22), 6233–6259. Taylor & Francis.

Kwak, M. (2018). Optimal line design of new and remanufactured products: A model for maximum profit and market share with environmental consideration. *Sustainability*, 10(11), 4283. MDPI.

Lambert, A. J. D. (2002). Determining optimum disassembly sequences in electronic equipment. *Computers & Industrial Engineering*, 43(3), 553–575. Elsevier.

Mazé, F. and Ahmed, F. (2022). Diffusion models beat GANs on topology optimization. *arXiv preprint, arXiv:2208.09591*.

Mooney, C. Z. (1997). *Monte Carlo Simulation*. Sage, No. 116.

Panagiotidou, S., Nenes, G., and Zikopoulos, C. (2013). Optimal procurement and sampling decisions under stochastic yield of returns in reverse supply chains. *OR Spectrum*, 35, 1–32. Springer.

Priyono, A., Ijomah, W., and Bititci, U. S. (2016). Disassembly for remanufacturing: A systematic literature review, new model development and future research needs. *Journal of Industrial Engineering and Management (JIEM*, 9(4), 899–932. Barcelona: OmniaScience.

Sadana, U., Chenreddy, A., Delage, E., Forel, A., Frejinger, E., and Vidal, T. (2024). A survey of contextual optimization methods for decision-making under uncertainty. European Journal of Operational Research. Elsevier.

Schlüter, M., Lickert, H., Schweitzer, K., Bilge, P., Briese, C., Dietrich, F., and Krüger, J. (2021). AI-enhanced identification, inspection and sorting for reverse logistics in remanufacturing. *Procedia CIRP*, 98, 300–305. Elsevier.

Sinaga, K. P. and Yang, M.-S. (2020). Unsupervised K-means clustering algorithm. *IEEE Access*, 8, 80716–80727. IEEE.

Sohl-Dickstein, J., Weiss, E., Maheswaranathan, N., and Ganguli, S. (2015). Deep unsupervised learning using nonequilibrium thermodynamics. *In Proceedings of the International Conference on Machine Learning*, 2256–2265. PMLR.

Sutton, R. S., Barto, A. G., *et al.* (1999). Reinforcement learning. *Journal of Cognitive Neuroscience*, 11(1), 126–134.

Stamer, F. and Sauer, J. (2024). Optimizing quality and cost in remanufacturing under uncertainty. *Production Engineering*, 1–22. Springer.

Sun, H. and Li, Y. (2023). Optimal acquisition and production policies for remanufacturing with quality grading. *Mathematics*, 11(7), 1665. MDPI.

Wahab, D. A., Blanco-Davis, E., Ariffin, A. K., and Wang, J. (2018). A review on the applicability of remanufacturing in extending the life cycle of marine or offshore components and structures. *Ocean Engineering*, 169, 125–133. Elsevier.

Wang, Z.-J., Zhou, R.-F., Ma, Y.-F., and Wang, Y.-J. (2024). Carbon tax and low-carbon credit: Which policy is more beneficial to the capital-constrained manufacturer's remanufacturing activities? *Environmental Research*, 246, 118079. Elsevier.

Yang, C.-H., Wang, J., and Ji, P. (2015). Optimal acquisition policy in remanufacturing under general core quality distributions. *International Journal of Production Research*, 53(5), 1425–1438. Taylor & Francis.

Zikopoulos, C. and Tagaras, G. (2007). Impact of uncertainty in the quality of returns on the profitability of a single-period refurbishing operation. *European Journal of Operational Research*, 182(1), 205–225. Elsevier.

Zhang, M., Amaitik, N., Wang, Z., Xu, Y., Maisuradze, A., Peschl, M., and Tzovaras, D. (2022). Predictive maintenance for remanufacturing based on hybrid-driven remaining useful life prediction. *Applied Sciences*, 12(7), 3218. MDPI.

Zheng, H., Li, E., Wang, Y., Shi, P., Xu, B., and Yang, S. (2019). Environmental life cycle assessment of remanufactured engines with advanced restoring technologies. *Robotics and Computer-Integrated Manufacturing*, 59, 213–221. Elsevier.

Zhang, X., Zhang, M., Zhang, H., Jiang, Z., Liu, C., and Cai, W. (2020). A review on energy, environment and economic assessment in remanufacturing based on life cycle assessment method. *Journal of Cleaner Production*, 255, 120160. Elsevier.